Strengthening Transmission System Resilience Against Extreme Weather Events by Undergrounding Selected Lines

Dimitris N. Trakas, *Member, IEEE*, and Nikos D. Hatziargyriou, *Life Fellow, IEEE*

***Abstract*—Natural disasters, such as extreme weather events (EWEs), can cause significant damage to power systems. In fact, it is expected that the intensity and frequency of EWEs will increase the next years due to climate change, making power system resilience enhancement necessary. This paper proposes a transmission resilience planning solution by determining the lines to be placed underground in order to minimize load shedding in the most cost-efficient way taking into account historical EWEs (HEWEs). The problem is formulated as a stochastic robust optimization problem and is decomposed into a master problem determining the lines to be placed underground and a number of subproblems, where each subproblem corresponds to a HEWE and provides the worst damage scenario that leads to the maximization of load shedding. The problem is solved using a decomposition-based algorithm. The proposed method is illustrated on a modified IEEE Reliability Test System and IEEE 118-bus System and it is evaluated by applying a Sequential Monte Carlo simulation.**

***Index Terms*—Extreme weather event, resilience, resiliency, stochastic robust optimization, transmission system planning, underground line.**

NOMENCLATURE

A. Indices, Sets and functions

e	Index for historical extreme weather events (HEWEs).
g	Index for generators.
i, j	Indices for buses.
(i,j)	Transmission line from bus i to bus j.
t	Index for time intervals.
$\mathcal{B}$	Set of buses.
$\mathcal{E}$	Set of HEWEs.
$\mathcal{G}$	Set of generators.
$\mathcal{G}_i$	Set of generators at bus i.
$\mathcal{L}$	Set of transmission lines.
$\mathcal{T}$	Set of time intervals for the examined period.
$\mathcal{T}_w$	Set of time intervals during extreme weather ($\mathcal{T}_w \subset \mathcal{T}$).
$\mathbb{D}_e$	Uncertainty set of damaged lines under e^{th} HEWE.
$\mathbb{O}_e$	Feasible system operation set under e^{th} HEWE.
$\mathbb{U}$	Feasible set of underground lines.
$C^{IC}()$	Investment cost function.
$C_e^{OC}()$	Operational cost function corresponding to the worst damage scenario under e^{th} HEWE.

B. Parameters

$c_{i,j}$	Cost of underground transmission line (i,j) [$].
D	Investment budget [$].
F^{EWE}	Estimated number of future extreme weather events (EWEs) during examined planning horizon.
M	Sufficiently big positive number.
$MTTR_{i,j}$	Mean time to repair line (i,j) [h].
$p_g^{G,max/min}$	Upper and lower generation limits of g^{th} generator [MW].
$p_{i,t}^L$	Demand active power of i^{th} bus at time interval t [MW].
$pf_{i,j}^{max/min}$	Upper and lower capacity limits of transmission line (i,j) [p.u.].
pr_e	Probability of future EWEs to be similar with e^{th} HEWE.
RU_g/RD_g	Ramp up/down rate of g^{th} generator [MW/h].
S_B	Base value of power [MVA].
T	Number of time periods in the optimization horizon.
T_w	Number of time periods during extreme weather ($T_w < T$).
$VoLL_i$	Value of lost load of i^{th} bus [$/MWh].
$X_{i,j}$	Reactance of transmission line (i,j) [p.u.].
$\vartheta^{max/min}$	Upper and lower limits of bus voltage angle [rad].
$\pi_{i,j,e,t}$	Damage probability of transmission line (i,j) under e^{th} HEWE at time interval t.

C. Variables

$k_{i,j,e,t}$	Binary variable indicating transmission line (i,j) damage under e^{th} HEWE at time interval t (1 in time interval of line damage, 0 otherwise).
$p_{g,e,t}^G$	Active power generation of g^{th} generator under e^{th} HEWE at time interval t [MW].

Manuscript received March 21, 2021; revised July 29, 2021; accepted November 8, 2021. Date of publication November 15, 2021; date of current version June 20, 2022. Paper no. TPWRS-00446-2021. *(Corresponding author: Dimitris N. Trakas.)*

Dimitris N. Trakas is with the Electric Power, National Technical University of Athens, 15780 Athens, Attiki, Greece (e-mail: dtrakas@power.ece.ntua.gr).

Nikos D. Hatziargyriou is with the Electrical and Computer Engineering, National Technical University of Athens, 15773 Athens, Greece (e-mail: nh@power.ece.ntua.gr).

Color versions of one or more figures in this article are available at https://doi.org/10.1109/TPWRS.2021.3128020.

Digital Object Identifier 10.1109/TPWRS.2021.3128020

$p^{shed}_{i,e,t}$ Active power shedding of i^{th} bus under e^{th} HEWE at time interval t [MW].

$pf_{i,j,e,t}$ Line active power flow of transmission line (i,j) under e^{th} HEWE at time interval t [p.u.].

$r_{i,j}$ Binary variable indicating if transmission line (i,j) is underground (1 underground, 0 otherwise).

$z_{i,j,e,t}$ Binary variable indicating if transmission line (i,j) is damaged under e^{th} HEWE at time interval t (1 non-damaged, 0 damaged).

$\vartheta_{i,e,t}$ Bus voltage angle of i^{th} bus under e^{th} HEWE at time interval t [rad].

$\boldsymbol{o}_e$ Matrix of system operation decision variables under e^{th} HEWE.

$\boldsymbol{r}$ Vector of decision variables $r_{i,j}$.

$\boldsymbol{z}_e$ Matrix of decision variables $z_{i,j,t}$ under e^{th} HEWE.

I. Introduction

EXTREME weather events have caused significant damages to power systems during the last decades, resulting in power outages for millions of customers. Prominent examples are hurricane Katrina that interrupted the power supply for more than 3.5 million of customers in 2005 [1] and superstorm Sandy that caused the disconnection of 8.5 million customers in 2012 [2], both in the USA. These and several other events have highlighted the necessity to enhance power system resilience, especially in view of the increased frequency of such extreme weather events (EWEs) due to climate change [3]. The term power system resilience is defined as the ability of the system to withstand, adapt and rapidly recover after the occurrence of high-impact, low-probability event, according to [4].

Conventional planning methods usually ignore the effect of EWEs, and natural disasters in general, on power systems. Hence, it is necessary to develop new planning methods assisting in determining the optimal hardening measures to enhance power system resilience against high-impact, low-probability events, such as natural disasters and malicious attacks. One of the most effective hardening measures to improve power system resilience is the installation of new lines or the enhancement of the existing ones. Various methods to determine the lines to be installed or enhanced have been proposed in the literature.

Stochastic optimization approaches have been proposed in [5]–[7]. In [5], a method optimizing the transmission and generation expansion planning to mitigate seismic impact on the power system is proposed. The impact of the earthquake on system components is modelled using fragility curves providing the probability of each component to be at a specific damage level. A two-stage stochastic programming is proposed in [6]. The line failure probabilities are obtained using fragility curves and the hardening measures are line enhancement, DGs installation and sectionalizers allocation. In [7] transmission network expansion is formulated as a problem of building new lines to mitigate the impact of potential attacks. A recursive method is applied to identify the worst damage scenarios for various numbers of destroyed lines and the probability of each scenario is estimated based on the damage caused and the number of destroyed lines. In stochastic optimization however, a limited number of scenarios is used in order to enable the solution of the problem in a reasonable time and this does not allow sufficient representation of the possible system degraded states, particularly when multiple potential threats are considered.

In [8] a heuristic method is proposed for the identification of the critical lines, in order to increase their robustness against EWEs. Fragility curves are used to obtain line failure probabilities due to extremely high wind speeds and a resilience index is defined which is used to sort the lines based on their criticality. However, heuristic methods do not guarantee the optimal solution.

The planner-attacker-defender model has been used in several papers to decide the optimal planning against external shocks. A method for the optimal installation of new transmission lines and switching devices for minimizing attacker impact is proposed in [9], modeling the attacker budget using the *N-k* criterion. In [10] distribution network planning against natural disaster is proposed which selects the optimal allocation of distributed generators and lines to be hardened. A multi-stage and multi-zone *N-k* criterion is applied to capture the impact of the natural disaster. A similar approach to model the impact of extreme events on system has been adopted in [11], which proposes a method to determine the line hardening and storage device deployment strategy. In [12] a method of selecting the buses and transmission lines to be protected against localized attacks is proposed. All the components within a circle shaped area under attack are considered damaged and the radius of the circle indicates attacker's budget. In [13] line hardening is determined considering the worst-case disruption scenario and the worst-case wind output. The failure probability of system components is ignored in [9]–[13] and therefore the impact on the power system might be over- or under-estimated.

A distribution system resilience hardening method is proposed in [14]. The hardening measures include upgrading poles and vegetation management under the worst damage scenario taking into account line failure probabilities. The problem is solved using a greedy searching algorithm. In [14], different hurricanes are examined separately, therefore an optimal hardening decision taking into account several hurricanes affecting different geographical areas of the system is not feasible. In [15], a data-driven transmission defense planning method based on distributionally robust optimization is presented. The model aims at determining the line hardening and new line construction to minimize extreme weather impact on power system. The probability of lines to fail are taken into account and the planning decision aims at minimizing expected system loss under the worst-case probability distribution of system failure states. The method proposed in [15] does not take into account the duration of the EWEs and requires the calculation of the probability of *k*-level failure states considering different hardening plans for each line before the solution of the optimization problem, which is time-costly, especially when the duration of the EWEs is considered.

This paper focuses on the selection of existing lines that should be placed underground in order to reduce load shedding with minimum investment costs in the event of extremely high wind speeds. Undergrounding lines is an effective measure against several, but not all natural disasters. It is effective against weather events characterized by extremely high wind speeds, such as hurricanes, typhoons and tornadoes [16]. It is also effective against ice storms, as the underground lines are protected from the weight of ice accumulated on the overhead lines or falling trees due to heavy snowfalls [17], and wildfires [16]. However, it is not effective against earthquakes [18] and precipitation-based hazards, such as floods which can damage non-submersible electrical equipment [19]. To reduce the vulnerability of underground lines against floods, they can be designed to operate while submerged in water, at increased investment cost [19]. Therefore, the implementation of such a measure should be determined taking into account the type of natural disasters threatening the geographical area under consideration.

Real-world projects have demonstrated the effectiveness of underground lines against hurricanes. Such projects are mainly found in distribution systems (e.g., [20], [21]). The results have shown that the customers have benefited from the minimization of damages and acceleration of the restoration process after a hurricane. Next to risk mitigation, line undergrounding has proven to be economically beneficial, considering the reduction of costs due to customer interruption and damage repair. Real-world projects in transmission systems are less frequent, although undergrounding of transmission lines has been proposed as a hardening measure to increase power system resilience in many reports [4], [16], [19], [22], [23]. As the cost of undergrounding transmission lines is much higher compared to overhead lines, the selection of critical transmission lines is of high importance [19], [23]. Moreover, underground lines take longer to restore and their repair costs are higher compared to overhead lines. This indicates the necessity of developing an effective method to determine the critical lines to be placed underground taking into account the tradeoff between costs due to the damages and investment costs. Despite the high cost of undergrounding, if the lines are selected properly, the reduction of operational cost due to the line damages provoked by EWEs could make the investment costs more efficient.

The main advantage of laying the lines underground is the elimination of line failure probabilities during EWEs, such as hurricanes, regardless of their intensity. On the contrast, the increase of towers' robustness, which is an effective hardening measure that can reduce the probability of tower collapses at a much lower cost compared to the cost for placing the lines underground, is not able to eliminate the line failure probability. For a given tower, even if its robustness has been enhanced, its failure probability increases as weather intensity increases. Given that the frequency and intensity of EWEs are expected to increase, underground lines can lead to a much higher reduction in the costs incurred after the occurrence of an EWE compared to increasing towers' robustness and therefore be a more economically viable solution.

In this paper, the resilience transmission planning problem is formulated as a multi-level stochastic robust optimization problem [24] that considers the impact of various Historical EWEs (HEWEs) on the system in order to determine which lines to place underground. A two-stage stochastic optimization is nested in the outer optimization problem to consider the probability of the future EWEs to be similar with one of the HEWEs under consideration and the robust optimization is nested in the inner optimization problem to hedge against the worst-case uncertainty realization regarding the line failures provoked by the HEWEs. The impact of the HEWEs on power system is modeled using fragility curves that provide the failure probabilities of the lines as a function of weather parameter intensity. The line failure probabilities are taken into account in order to minimize the operational cost under the worst damage scenario identified by the robust optimization considering only the system degraded states with probability over a predefined threshold. The threshold depends on the system operator and indicates the security criteria to be fulfilled.

Compared to the stochastic optimization approaches proposed in [5]–[7], the formulation of the inner robust problem enables the consideration of multiple EWEs taking into account all possible system degraded states with a probability over the predefined threshold set by the operator during an EWE, while the problem is solved in a reasonable time. In addition, compared to the planner-attacker-defender models proposed in [9]–[13], the inner robust problem takes into account the line failure probabilities. In contrast to the heuristic methods presented in [8], the proposed method guarantees the optimal solution. Compared to [14], the outer stochastic optimization allows the consideration of multiple EWEs, taking also into account their occurrence probability. Moreover, the proposed method does not require any calculations before the execution of the optimization problem, as in [15] which requires the calculation of the probability of k-level failure states considering different hardening plans for each line. Taking into account that the proposed model considers the duration of the EWEs and not just the possible system degraded states at the end of the EWEs as in [15], these calculations would be extremely time-costly, as the scenarios at each time interval depends on the line failures of the previous ones increasing the possible scenarios at each time interval dramatically.

The formulation of the robust inner optimization problem is based on [25], which proposes a method to determine the optimal unit commitment in case of an imminent EWE. Compared to [25], the problem in this paper is formulated as a multi-level stochastic robust optimization problem enabling the consideration of multiple HEWEs and providing an optimal selection of lines to be placed underground in a reasonable time. In addition, it allows to take into account the probability of the future EWEs to be similar with one of the HEWEs under consideration, as well as the line failure probabilities during EWEs.

The proposed problem is decomposed into a master problem and several subproblems and solved using a decomposition-based algorithm. The master problem provides the optimal planning by selecting the lines to be placed underground and each subproblem corresponds to a HEWE identifying the damage scenario that leads to the maximum load shedding cost. The

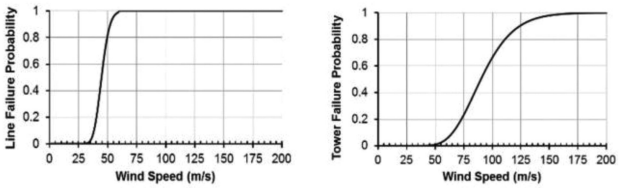

Fig. 1. Wind fragility curves.

decomposition-based algorithm iteratively solves the master problem and the subproblems and adds the worst damage scenario of each HEWE to the master problem at each iteration, until the relative optimality gap is reduced to the predefined tolerance.

The main contributions of this paper are:

- A resilient planning method is proposed for the determination of the lines to be placed underground, so as to enhance power system resilience considering multiple HEWEs and providing an optimal solution in reasonable time.
- A stochastic robust optimization problem is proposed to consider the uncertainty of a future EWE to be similar with one of the HEWEs under consideration and of the line failures provoked by them.
- The problem is reformulated as a two-stage problem and a decomposition-based algorithm is developed to solve it.

The rest of this paper is organized as follows: Section II describes the methodology used to model the impact of the weather event on power system components. Section III presents the problem framework and mathematical formulation, as well as the solution algorithm. Section IV presents the numerical results and evaluates the effectiveness of the proposed method. Section V concludes the paper.

II. Modeling the Impact of the Weather Event

It is assumed that only the overhead lines are affected by EWEs, while the substations and underground lines are not affected. It is considered that an overhead line can fail due to a direct failure of the line or a tower collapse across the line. Fragility curves are used to quantify the impact of extreme weather on the affected components at each simulation step. The fragility curves express the weather-dependent failure probability of a component as a function of the weather parameter, such as the wind speed [26]. The curves used are presented in Fig. 1.

It is noted that a different fragility curve could be used for each line and tower, if they are available. For simplicity, in this paper, the fragility curves presented in Fig. 1 are used for all the lines and towers. Considering that an overhead line can fail due to a direct failure of the line or a tower collapse across the line the failure probability, $\pi_{i,j}$, of line (i,j) is given by [26]:

$$\pi_{i,j} = \pi_{i,j,tower} + \pi_{i,j,line} - \pi_{i,j,tower}\pi_{i,j,line} \quad (1)$$

$\pi_{ij,line}$ is the probability of line (i,j) to fail due to a direct line failure and is obtained by the line fragility curve directly. $\pi_{ij,tower}$ is the probability of line (i,j) to fail due to a tower collapse across the line. According to various studies, the failure of a high-voltage transmission tower due to the mechanical forces exercised by the failure of an adjacent tower, is extremely uncommon [8], [27], [28]. Therefore, considering that the failure of a tower is independent from the failure of the other towers across the same line, $\pi_{i,j,tower}$ is calculated as follows [8]:

$$\pi_{i,j,tower} = 1 - \prod_{b=1}^{N_T} (1 - \pi_{b,tower}) \quad (2)$$

where $\pi_{b,tower}$ is the failure probability of tower b, obtained by the tower fragility curve, and N_T is the number of towers across line i,j. It is assumed that for each line there is one tower per 300m connected in series and therefore the number of towers across a line can be calculated based on the length of the line [26].

Assuming that k line failures can occur at the same time interval, the probability of the degraded system state is given by:

$$\pi\left(\bigcap_{m\in\boldsymbol{K}} l_m\right) = \prod_{m\in\boldsymbol{K}} \pi(l_m) \prod_{n\in\mathcal{L}-\boldsymbol{K}} (1-\pi(l_n)) \quad (3)$$

where $\boldsymbol{K}$ is the set of damaged lines and $\pi(l_m)$ is the failure probability of line l_m obtained from (1).

III. Problem Formulation

A. Model Overview

Two sources of uncertainty are considered in this paper. The uncertainty of a future EWE to be similar with one of the HEWEs under consideration and the uncertainty of line failures during an EWE. In order to deal with these uncertainties, two-stage stochastic programming and robust optimization are combined. The aim is to find a solution that performs well for all future EWEs that are similar to those in the past. The framework of the problem, when N HEWEs are considered, is presented in Fig. 2.

A two-stage stochastic optimization is nested in the outer problem to optimize the investment and expected operational costs under the worst-case scenario of each HEWE taking into account the probability of the future EWEs to be similar with one of the HEWEs under consideration. The objective is to determine which lines should be placed underground, $\boldsymbol{r}$, to minimize the investment cost and the second-stage expected operational costs under the worst-case scenario for each HEWE.

A robust optimization is nested in the inner optimization problem to hedge against the worst-case uncertainty realization regarding the line failures provoked by the HEWEs. The robust optimization is used to deal with the high-dimensional uncertainty of line damages, aiming to provide a good balance between solution quality and computational tractability. For each HEWE, the robust optimization is formulated as a max-min bi-level optimization problem. The first level determines the line damages, $\boldsymbol{z}_e$, that maximize the operational cost and the second level determines the system operation, $\boldsymbol{o}_e$, that minimizes the operational cost under the worst-case scenario. The worst-case scenario is determined taking into account the security criteria that need to be fulfilled, which are set by the system operator.

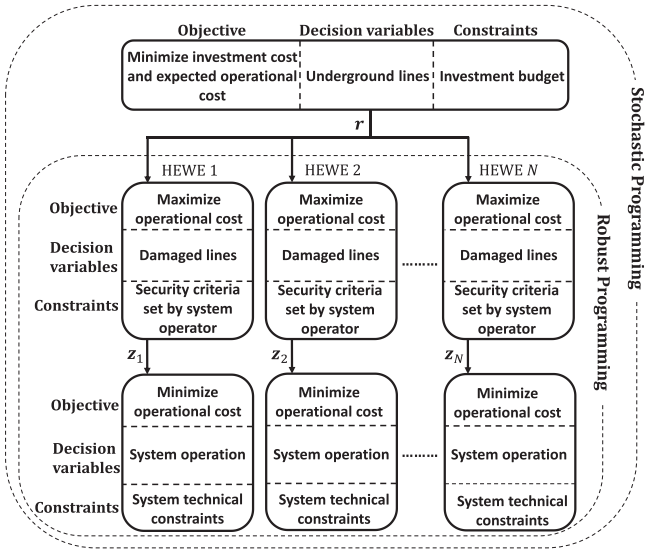

Fig. 2. Framework of the proposed optimization problem.

Their modeling is described in Section III-B. The system operation is determined taking into account the system technical constrains.

B. Mathematical Formulation

The outer two-stage stochastic optimization problem is formulated as follows:

$$\min_{\boldsymbol{r}\in\mathbb{U}} C^{IC}(\boldsymbol{r}) + F^{EWE}\mathbb{E}_{e\in\mathcal{E}}\left[\overline{C_e^{OC}}(\boldsymbol{r})\right] \tag{4}$$

$$C^{IC}(\boldsymbol{r}) = \sum_{(i,j)\in\mathcal{L}} c_{i,j} r_{i,j} \tag{5}$$

$$\mathbb{U} = \left\{ \boldsymbol{r} \,\middle|\, \sum_{(i,j)\in\mathcal{L}} c_{i,j} r_{i,j} \le D \right\} \tag{6}$$

The objective function (4) aims at minimizing the investment cost and the expected operational cost during the planning horizon, considering the worst damage scenario of each HEWE under consideration. Considering the investment cost in the objective function ensures not only that the most cost-efficient solution is provided, but also that the minimum number of underground lines is selected. The investment cost is equal to the cost of placing lines underground, as presented in (5). Constraint (6) guarantees that this cost does not exceed the investment budget.

Assuming that pr_e is the probability of a future EWE to be similar to the e^{th} HEWE under consideration and $\sum_{e\in\mathcal{E}} pr_e = 1$, (4) is expressed as:

$$\min_{\boldsymbol{r}\in\mathbb{U}} C^{IC}(\boldsymbol{r}) + F^{EWE}\sum_{e\in\mathcal{E}} pr_e \overline{C_e^{OC}}(\boldsymbol{r}) \tag{7}$$

These probabilities can be calculated based on how many times a geographical region has experienced EWEs in relation to the total number of EWEs, and in the context of robust optimization, the HEWE that has caused the worst damage can be used to determine the optimal system planning. Alternatively, all the HEWEs can be considered and $pr_e = 1/\#\mathcal{E}$, where $\#\mathcal{E}$ is the cardinality of $\mathcal{E}$.

The operational cost that corresponds to the worst damage scenario under the e^{th} HEWE is given by:

$$\begin{aligned}\overline{C_e^{OC}}(\boldsymbol{r}) &= \max_{\boldsymbol{z}_e\in\mathbb{D}_e(\boldsymbol{r})} \min_{\boldsymbol{o}_e\in\mathbb{O}_e(\boldsymbol{z}_e,\boldsymbol{r})} C_e^{OC}(\boldsymbol{r},\boldsymbol{z}_e,\boldsymbol{o}_e) \\ &= \max_{\boldsymbol{z}_e\in\mathbb{D}_e(\boldsymbol{r})} \min_{\boldsymbol{o}_e\in\mathbb{O}_e(\boldsymbol{z}_e,\boldsymbol{r})} \sum_{t\in\mathcal{T}}\sum_{i\in\mathcal{B}} VoLL_i p_{i,e,t}^{shed}\end{aligned} \tag{8}$$

As shown in (8), the operational cost is equal to the load shedding cost. The repair cost of the damaged lines could be also added to the operational cost. However, it is much lower than the cost of placing the lines underground. As a result, it is not economically beneficial to place a line underground just to avoid the repair cost. The consideration of the repair cost could affect the selection of which lines are placed underground in very specific cases. In particular, it could affect the decision to underground a line, only if its placement underground results in a reduction in the load shedding cost slightly lower than the investment cost of placing the line underground. The consideration of the repair cost in this case could result in a reduction of load shedding and repair costs, due to the undergrounding of the line, that is slightly higher compared to the investment cost. Therefore, the undergrounding of the line due to the consideration of the repair cost in the objective function would not have a significant impact on the total cost consisting of investment, load shedding and repair costs.

The constraints of the inner robust optimization problem for the e^{th} HEWE are the following:

$$\mathbb{D}_e(\boldsymbol{r}) = \left\{ \boldsymbol{z}_e \,\middle|\, \prod_{(i,j)\in\mathcal{L}} \left(\pi_{i,j,e,t}{}^{k_{i,j,e,t}}(1-\pi_{i,j,e,t})^{z_{i,j,e,t}}\right) \ge \pi_{thres},\ \forall t\in\mathcal{T}_{\boldsymbol{w}} \right. \tag{9}$$

$$z_{i,j,e,t} \le z_{i,j,e,t-1},\ \forall (i,j)\in\mathcal{L},\ t\in\mathcal{T}_{\boldsymbol{w}} \tag{10}$$

$$k_{i,j,e,t} = z_{i,j,e,t-1} - z_{i,j,e,t},\ \forall (i,j)\in\mathcal{L},\ t\in\mathcal{T}_{\boldsymbol{w}} \tag{11}$$

$$z_{i,j,e,t} \ge r_{i,j},\ \forall (i,j)\in\mathcal{L},\ t\in\mathcal{T} \tag{12}$$

$$\left. z_{i,j,e,t} = z_{i,j,e,T_w},\ \forall (i,j)\in\mathcal{L},\ t\in[T_w+1, T_w+MTTR_{i,j}] \right\} \tag{13}$$

$$\mathbb{O}_e(\boldsymbol{z}_e,\boldsymbol{r}) = \left\{ \boldsymbol{o}_e \,\middle|\, p_{i,t}^L \le \sum_{g\in\mathcal{G}_i} p_{g,e,t}^G + p_{i,e,t}^{shed} - S_B\left(\sum_{\{j|(i,j)\in\mathcal{L}\}} pf_{i,j,e,t} - \sum_{\{j|(j,i)\in\mathcal{L}\}} pf_{ji,e,t}\right) \le p_{i,t}^L, \right.$$
$$\forall i\in\mathcal{B},\ t\in\mathcal{T} \tag{14}$$

$$p_g^{G,min} \le p_{g,e,t}^G \le p_g^{G,max},\ \forall g\in\mathcal{G},\ t\in\mathcal{T} \tag{15}$$

$$p_{g,e,t-1}^G - p_{g,e,t}^G \ge -RU_g,\ \forall g\in\mathcal{G}, t\in\mathcal{T} \tag{16}$$

$$p^G_{g,e,t} - p^G_{g,e,t-1} \geq -RD_g,\ \forall g \in \mathcal{G}, t \in \mathcal{T} \tag{17}$$

$$pf^{min}_{i,j} z_{i,j,e,t} \leq pf_{i,j,e,t} \leq pf^{max}_{i,j} z_{i,j,e,t} \quad \forall (i,j) \in \mathcal{L},\ t \in \mathcal{T}, \tag{18}$$

$$-(1 - z_{i,j,e,t})\, M_1 \leq pf_{i,j,e,t} - \frac{(\vartheta_{i,e,t} - \vartheta_{j,e,t})}{X_{i,j}} \leq (1 - z_{i,j,e,t})\, M_1,\ \forall (i,j) \in \mathcal{L}, t \in \mathcal{T} \tag{19}$$

$$\vartheta^{min} \leq \vartheta_{i,e,t} \leq \vartheta^{max},\ \forall i \in \mathcal{B},\ t \in \mathcal{T} \tag{20}$$

$$0 \leq p^{shed}_{i,e,t} \leq p^L_{i,t},\ \forall i \in \mathcal{B},\ t \in \mathcal{T} \Big\} \tag{21}$$

Using constraint (9), only the degraded system states due to line damages with probability over a predefined threshold π_{thres} at each time interval during extreme weather are considered. The selection of π_{thres} value depends on the security criteria to be fulfilled. The lower the value, the lower the probability of the degraded system states considered and therefore system states leading to higher load shedding are considered. More details can be found in [25]. Constraint (10) guarantees that if a line is damaged due to extreme weather, it will remain off-line up to the end of extreme weather, as it is assumed that restoration is not possible during the event, mainly due to safety reasons [29]. Constraint (11) specifies that the binary variable $k_{i,j,e,t}$ becomes equal to 1, only in the time interval t the line (i,j) is damaged. Constraints (9)-(11) can be used to take into account the degraded system states during an EWE so as to determine the optimal operation or hardening measures to increase power system resilience. For instance, in [25], these constraints are used to determine the optimal unit commitment in case of an imminent EWE, while in this paper, they are used to determine which lines to be placed underground considering the impact of multiple HEWEs. Constraint (12) assures that if a line is underground, it cannot be damaged by the EWE. Constraint (13) guarantees that if a line is damaged, it will remain off-line until it is restored. It is assumed that there are enough repair crews in order to repair all damaged lines simultaneously. The optimization problem does not distinguish if a line fails due to direct failure or due to a tower collapse across the line. Therefore, the Mean Time to Repair ($MTTR$) of a damaged line should be selected taking into account both cases, as well as the probability of them. It is noted that the difficulties of restoring a line after an EWE should be considered when determining the $MTTR$. In general, the restoration time after an EWE depends on several factors such as the the type of the damaged component, the severity of the extreme weather which affects the level of damage, the number of the repair crews that are assigned to each damaged component, the training received from the repair crews and their experience, the availability of critical equipment and components to repair the damage and the time required to approach the damaged component. Although a simplified modeling of repair procedure is considered in this paper, it does not affect the selection of the lines to be placed underground, which is the focus of this paper.

Power balance, generation limits and upward and downward ramping constraints are described by (14), (15), (16) and (17), respectively. Constraint (14) could be expressed as an equality. It is expressed as two inequalities in order to provide a problem formulation consistent with the generic problem expression presented in Section III-C. Using constraint (18), power flow through the line is allowed only when the line is functional. DC power flow equations are represented by (19). Equation (19) is converted to equality when the line is functional and relates phase angles to power flow. M_1 is activated when the lines are outaged and is suitably selected in order to allow the calculation of phase angles of the buses at the ends of lines set out of order. Constraints (20) and (21) represent the phase angle limits and load shedding bounds, respectively.

C. Problem Reformulation

Considering that $\hat{\boldsymbol{r}}$ is the planning decision, the failure probability of the underground lines can be set equal to the failure probability under normal operating conditions regardless the prevailing weather. Given that the line failure probability under normal conditions is lower than threshold π_{thres} and therefore the underground lines cannot be damaged due to EWE, (12) can be omitted.

By linearizing (9), taking the logs of both sides [25], the max-min problem of the inner robust optimization problem under the e^{th} HEWE can be expressed as follows:

$$\max_{\boldsymbol{z}_e \in \mathbb{D}_e(\hat{\boldsymbol{r}})} \min_{\boldsymbol{o}_e \in \mathbb{O}(\boldsymbol{z}_e, \hat{\boldsymbol{r}})} \boldsymbol{v}^\top \boldsymbol{o}_e \tag{22}$$

$$s.t.\ \ \boldsymbol{A}\boldsymbol{o}_e + \boldsymbol{B}\hat{\boldsymbol{r}} + \boldsymbol{E}\boldsymbol{z}_e \geq \boldsymbol{F} \tag{23}$$

$$\boldsymbol{G}\boldsymbol{z}_e \geq \boldsymbol{K} \tag{24}$$

where, $\boldsymbol{A}$, $\boldsymbol{B}$, $\boldsymbol{E}$ and $\boldsymbol{F}$ are matrices used to describe constraints (14)-(21). $\boldsymbol{G}$ and $\boldsymbol{K}$ are the matrices used to describe constraints (9)-(13). $\boldsymbol{v}$ is the matrix describing the load shedding costs.

The max-min problem can be converted into a max problem considering the dual formulation of the inner optimization problem of (22) which is a linear problem with respect to $\boldsymbol{o}_e$.

$$\max_{\boldsymbol{z}_e \in \mathbb{D}_e(\hat{\boldsymbol{r}})} \max_{\boldsymbol{\lambda}_e \in \mathbb{F}(\boldsymbol{z}_e, \hat{\boldsymbol{r}})} (\boldsymbol{F} - \boldsymbol{B}\hat{\boldsymbol{r}} - \boldsymbol{E}\boldsymbol{z}_e)^\top \boldsymbol{\lambda}_e \tag{25}$$

$$s.t.\ \boldsymbol{A}^\top \boldsymbol{\lambda}_e \leq \boldsymbol{v} \tag{26}$$

$$\boldsymbol{G}\boldsymbol{z}_e \geq \boldsymbol{K} \tag{27}$$

where $\boldsymbol{\lambda}_e$ is the matrix describing the dual variables of constraints (14)-(21) and $\mathbb{F}(\boldsymbol{z}_e, \hat{\boldsymbol{r}})$ is the set of feasible solutions of the dual problem corresponding to the e^{th} HEWE. It is observed that objective function of the dual problem contains bi-linear terms due to the multiplication of $\boldsymbol{z}_e$ with $\boldsymbol{\lambda}_e$. These terms are linearized according to the method described in [25]. In this way, the max-min problem of the inner robust optimization problem is reformulated to a maximization problem.

D. Solution Algorithm

The problem shown in (4) is decoupled into a master problem and a number of subproblems, where each subproblem corresponds to a HEWE. The master problem determines the optimal planning, while the subproblems identify the line failures that lead to the maximum operational cost. A customized Column & Constraint Generation (C&CG) algorithm is used to solve the problem [24]. The worst damage scenario that is determined by

each subproblem is iteratively added to the master problem until an optimal solution is found. It is noted that the subproblems corresponding to HEWEs can be solved in parallel at each iteration of the decomposition algorithm reducing the execution time of the method. The algorithm termination within finite iterations is guaranteed due to the finite number of extreme points of the uncertainty sets $\mathbb{D}_e$. In order to apply C&CG, the subproblem must be feasible. By considering load shedding, the subproblem is feasible for all considered HEWEs in all iterations of the algorithm, regardless the damaged lines.

Hence, the master problem considers a set of worst damage scenarios $\hat{\mathbb{D}}_e = \{\hat{\boldsymbol{z}}_e^l,\ l = 1, \ldots, m\}$ for each HEWE at iteration l and is expressed as:

$$\min_{\boldsymbol{r}\in\mathbb{U},\ \boldsymbol{o}_e^l\in\mathbb{O}\left(\hat{\boldsymbol{z}}_e^l,\boldsymbol{r}\right)} C^{IC}\left(\boldsymbol{r}\right) + F^{EWE}\varphi \tag{28}$$

$$s.t\ \varphi \geq \sum_{e\in\mathcal{E}}\left(pr_e \arg\max_l C_e^{OC}\left(\boldsymbol{o}_e^l\right)\right),\quad \forall l \in 1, \ldots, m \tag{29}$$

$$\boldsymbol{A}\boldsymbol{o}_e^l + \boldsymbol{B}\boldsymbol{r} + \boldsymbol{E}\hat{\boldsymbol{z}}_e^l \geq \boldsymbol{F},\ \forall e \in \mathcal{E},\ l \in 1,\ \ldots,\ m \tag{30}$$

where φ is a scalar variable introduced to guarantee that the optimal solution of the master problem dominates expected operational cost corresponding to the included worst damage scenarios. It is noted that the worst damage scenario of each HEWE can be detected at a different iteration l.

Given that the master problem considers a restricted set of worst damage scenarios provided by the subproblems and that the optimal solution provided is lower than the one for the complete set of feasible damage scenarios, it provides a lower bound (LB) of the original problem. Solving the subproblem, using the solution provided at iteration l, $\hat{\boldsymbol{r}}^l$, the worst damage scenario corresponding to each HEWE that maximizes the operational cost is provided. The expected operational cost, considering all the HEWEs plus the investment cost, provide an upper bound (UB) of the original problem. The line failure probabilities are updated at each iteration based on the master problem decision $\hat{\boldsymbol{r}}^l$. In particular, the failure probabilities of the underground lines are set equal to the failure probability under normal conditions regardless of whether they are located within the area affected by the extreme weather. The above steps are repeated until the difference between UB and LB is lower than a predefined optimality gap ε. The C&CG algorithm has been also used in [25] in order to determine the optimal unit commitment in case of an imminent EWE. Since only one EWE is considered in [25], the relevant subproblem is solved once at each iteration of the C&CG algorithm. In this paper, at each iteration, the subproblem is solved for each HEWE separately and the expected load shedding is calculated based on the probabilities pr_e. Moreover, in this paper, the line failure probabilities are updated at each iteration based on which lines have been placed underground. This does not apply in [25], as hardening measures are not examined and therefore the line failure probabilities do not change.

Algorithm 1 describes the detailed approach. $\hat{\mathbb{D}}_e$ is a set of worst damage scenarios of the e^{th} HEWE and $\hat{\boldsymbol{o}}_e^l$ is the system operation decision under e^{th} HEWE at iteration l. $\hat{\boldsymbol{z}}_e^l$ is the worst damage scenario of the e^{th} HEWE that leads to the highest operational cost at iteration l. It is noted that in the first iteration the master problem is solved considering all the lines in operation.

Algorithm 1 Customized C&CG Decomposition Approach

{Set all lines functional}
$LB \leftarrow -\infty$, $UB \leftarrow \infty$, $l \leftarrow 1$, $\hat{\mathbb{D}}_e \leftarrow \emptyset\ \forall e \in \mathcal{E}$ and
$\varepsilon \leftarrow 0.001$
while $|\frac{UB-LB}{UB}| > \varepsilon$ **do**
  {Solve master problem presented in (28)-(30) to obtain $\hat{\boldsymbol{r}}^l$}
  {Update line failure probabilities based on $\hat{\boldsymbol{r}}^l$}
  $LB \leftarrow \max(LB, C^{IC}(\hat{\boldsymbol{r}}^l) + F^{EWE}\hat{\varphi})$
  for $e = 1$ to $\#\mathcal{E}$ do
    {Solve the subproblem presented in (25)-(27) for the e^{th} HEWE to obtain $\hat{\boldsymbol{z}}_e^l$ and $\hat{\boldsymbol{o}}_e^l$}
    $\hat{\mathbb{D}}_e \leftarrow \hat{\boldsymbol{z}}_e^l \cap \hat{\mathbb{D}}_e$
  end for
  $UB \leftarrow$
  $\min(UB, C^{IC}(\hat{\boldsymbol{r}}^l) + F^{EWE}\sum_{e\in\mathcal{E}} pr_e C_e^{OC}(\hat{\boldsymbol{o}}_e^l))$
  $l \leftarrow l + 1$
end while
return $\hat{\boldsymbol{r}}$ and UB

IV. Case Study Application

This section presents the numerical results of the proposed method applied to a modified IEEE Reliability Test System [30] shown in Fig. 3 and IEEE 118-bus System [31]. It is considered that all the lines are overhead and the transformers are not affected by the EWEs. The duration of the HEWEs is considered equal to one day (24 hours). The restoration starts after the end of the EWEs and the $MTTR$ of a damaged line is considered equal to 50 hours. Hence, the total simulation time is 24+50 = 74 hours with an hourly resolution. The $MTTR$ has been determined based on the statistics of outages due to wind for the period 1999-2008 presented in [32] and the $MTTR$ used in [8]. Five HEWEs, presented in Fig. 4, are considered in this study. It is noted that the simultaneous occurrence of any of these HEWEs is not considered. The cost of placing the existing lines underground is considered equal to 0.5 and 1.24 \$·10^6/km for 138 kV and 230 kV lines, respectively. The cost of undergrounding the lines depends heavily on the terrain characteristics of the area. Digging the soil in some areas might be a demanding task, increasing significantly the cost of placing the lines underground, or it might be even an impossible task. This should be taken into account in a real-life application. The value of lost load is set at 20,000 \$/MWh [33].

The proposed model is implemented in YALMIP package with Gurobi solver. A PC with Intel Core i7 @3.40GHz and 16 BG RAM was used. The predefined optimality gap ε is selected equal to 0.001.

A Sequential Monte Carlo (SMC) simulation is used in order to evaluate the effectiveness of the proposed method. During

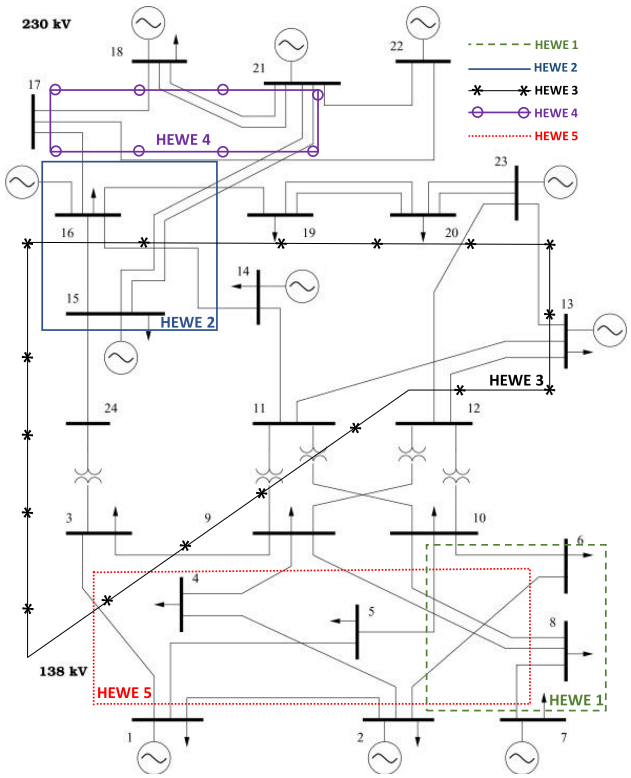

Fig. 3. IEEE Reliability Test System and affected areas by HEWEs.

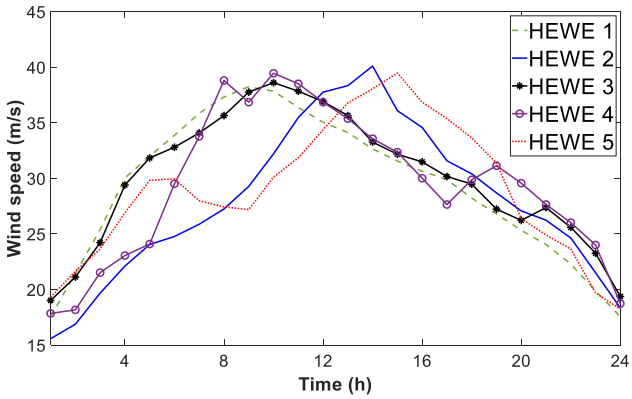

Fig. 4. Wind profiles of HEWEs.

SMC simulation, the underground lines determined by the proposed optimization problem are used as input and the problem that minimizes the operational cost is solved. At each iteration of the SMC simulation a random binary number based on the probabilities pr_e is generated to select a HEWE. Then the failure probabilities of the lines that are calculated based on their fragility curves and the HEWE under consideration are compared with a uniformly distributed random number $y \sim U(0,1)$ to decide their status at each time step. If the failure probability of the line is larger than y , then it is tripped. If a line is damaged, it will remain off-line until it is restored. It is noted that π_{thres} in (9) is used in order to allow the operator to consider in the optimization problem only the line failures with probability higher than a predefined threshold. This does not imply that during SMC simulation failures with lower probability than this threshold do not occur, but the line failures considered are obtained only from the comparison between their failure probabilities, obtained by fragility curves, and the randomly generated numbers y.

TABLE I
LINES EXPOSED TO EACH HEWE – IEEE RELIABILITY TEST SYSTEM

HEWE	Vulnerable lines
1	B2-B6, B5-B10, B6-B10, B7-B8, B8-B9, B8-B10
2	B14-B16, B15-B16, B15-B24, B16-B17, B16-B19, B15-B21(double)
3	B1-B3, B3-B9, B11-13, B11-B14, B12-13, B12-B23, B13-B23, B14-B16, B15-B16, B15-B21 (double), B15-B24
4	B16-B17, B17-B18, B17-B22, B18-B21 (double), B15-B21(double)
5	B1-B2, B1-B3, B1-B5, B2-B4, B2-B6, B4-B9, B5-B10, B7-B8, B8-B9, B8-B10

A. *Modified IEEE Reliability Test System*

The system is composed of 14 generators, 24 buses and 38 transmission lines. The hourly load demand is adopted from [34]. The investment budget is set to 12.5 $\cdot 10^7$ \$. The examined planning horizon is considered equal to 20 years and the expected number of EWEs during this period equal to 4. Hence, an average of one EWE every 5 years is assumed. The value of F^{EWE} can be selected based on the occurrence frequency of HEWEs or selected slightly higher to capture the increasing occurrence frequency of EWEs due to climate change. The probabilities of a future EWE to be similar with one of the HEWEs under consideration are considered equal. Therefore $pr_e = 1/5 = 0.2$ for all the HEWEs.

The affected areas by the wind profiles are presented in Fig. 3. The lines included within the areas presented in Fig. 3 are the ones exposed to the wind profiles presented in Fig. 4. The weather characteristics are assumed homogenous within each affected area and therefore the system components within an area are exposed to the same weather conditions. For example, regarding HEWE 1, the vulnerable lines are B2-B6, B5-B10, B6-B10, B7-B8, B8-B9 and B8-B10 and they are all exposed to the wind profile of HEWE 1 presented in Fig. 4. Table I presents the lines exposed to each HEWE. Their failure probabilities are calculated based on the fragility curves and the related wind profile. For each HEWE, the failure probability of all the lines outside the affected area is equal to the one under normal conditions, that is taken as 0.01% for overhead lines and 0.001% for underground lines.

It is noted that the parallel lines are examined separately in this paper. It is assumed that the parallel lines sharing the same towers are represented by an equivalent line, while the parallel lines carried by different towers are represented by different lines, e.g., those between buses 20 and 23 (B20-B23). The latter can follow different routes either due to geographical restrictions or for reliability reasons. For instance, parallel lines could be placed at a safe distance so that they are not threatened by the same exogenous threats. Therefore, placement of only one of the two

TABLE II
SMC SIMULATION RESULTS FOR CASE I WHEN $F^{EWE} = 4$

π_{thres} (%)	Underground Lines	Investment Cost ($\$ \times 10^7$)	LS Cost ($\$ \times 10^7$)	SMC Iter. with LS (%)	Total Cost ($\$ \times 10^7$)
1 & 3	B1-B5, B3-B9, B4-B9, B6-B10, B7-B8, B11-B13, B11-B14, B14-B16, B15-B21	11.173	0	0	11.173
5	B6-B10, B7-B8, B15-B16	1.661	2.213	20.2	10.513
>5	-	-	3.387	26.8	13.548

parallel lines underground is allowed. However, the optimization problem can be easily modified so as only the placement of both lines underground is allowed, regardless if they share same towers or not.

In order to verify the effectiveness of the proposed method, four cases are considered:

Case I: The wind profiles shown in Fig. 4 are used and the selection of the predefined threshold π_{thres} is investigated.

Case II: The wind profiles of the HEWEs are scaled-up and -down (the wind speed of all time intervals is multiplied by a constant number) to consider more and less extreme events. By scaling-up the wind profiles of HEWEs, the increasing intensity of EWEs due to climate change can be simulated.

Case III: Different probabilities of a future EWE to be similar with one of the HEWEs are examined. The performance of the proposed method is also compared with that of a stochastic optimization model.

Case IV: Different investment budgets are investigated to determine the optimal one.

1) Case I: Using the underground lines provided by the optimization problem, its effectiveness is evaluated executing the SMC simulations. The results for different values of π_{thres}, using a step of 2%, are presented in Table II. The last row shows the results for π_{thres} higher than 5%. In this case, no line is placed underground and therefore no investment is made. For π_{thres} equal to 1% and 3%, the same lines are determined to be placed underground. The second column shows the underground lines, while the third one shows the investment cost for placing them underground. The fourth column shows the average load shedding (LS) cost of the SMC simulation. The fifth column shows the percentage of SMC iterations with load shedding higher than zero. The total cost considering 4 EWEs during the examined planning horizon ($F^{EWE} = 4$) is presented in the last column and is equal to the investment cost plus the LS cost, presented in the fourth column, multiplied by F^{EWE}. It is highlighted that the underground lines and the investment cost result from the solution of the optimization problem, while the LS cost and the number of iterations with LS are results of the SMC simulation, using the underground lines provided by the optimization problem.

TABLE III
TOTAL COST FOR *CASE I* WHEN $F^{EWE} = 5$

π_{thres} (%)	1 & 3	5	>5
Total Cost ($\$ \times 10^7$)	11.173	12.726	16.935

TABLE IV
SMC SIMULATION RESULTS FOR CASE II WHEN $F^{EWE} = 4$ (WIND PROFILES SCALED-UP BY 2%)

π_{thres} (%)	Underground Lines	Investment Cost ($\$ \times 10^7$)	LS Cost ($\$ \times 10^7$)	SMC Iter. with LS (%)	Total Cost ($\$ \times 10^7$)
1 & 3	B1-B5, B3-B9, B4-B9, B6-B10, B7-B8, B11-B13, B11-B14, B14-B16, B15-B21	11.173	0	0	11.173
5	B1-B5, B6-B10, B7-B8, B15-B16	2.990	3.578	25.1	17.302
7	B6-B10, B7-B8, B15-B16	1.661	4.131	32.2	18.185
> 7	-	-	6.814	47.0	27.256

TABLE V
SMC SIMULATION RESULTS FOR CASE II WHEN $F^{EWE} = 4$ (WIND PROFILES SCALED-DOWN BY 2%)

π_{thres} (%)	Underground Lines	Investment Cost ($\$ \times 10^7$)	LS Cost ($\$ \times 10^7$)	SMC Iter. with LS (%)	Total Cost ($\$ \times 10^7$)
1	B1-B5, B3-B9, B4-B9, B6-B10, B7-B8, B11-B13, B11-B14, B14-B16, B15-B21	11.173	0	0	11.173
3	B1-B5, B3-B9, B4-B9, B6-B10, B7-B8, B11-B14, B14-B16, B15-B24	9.122	0.243	6.2	10.094
5	B6-B10, B7-B8	0.868	0.879	11.8	4.384
>5	-	-	1.368	14.6	5.472

The contribution of underground lines to power system resilience against EWEs of high wind speed is revealed by comparing the total cost. When the proposed method is applied, the total cost reduces for all the examined values of π_{thres}. As it was expected, as π_{thres} decreases, more lines are placed underground and the investment cost increases. This happens because as π_{thres} decreases a higher number of line failures is taken into account. The lowest total cost is observed for π_{thres} equal to 5%. However, load shedding is carried out in 20.2% of the SMC iterations. Therefore, if the operator aims to minimize the load shedding, the selected π_{thres} should be lower than 5%.

Table III shows the results when F^{EWE} is equal to 5. In this case, the lowest total cost is detected for π_{thres} values lower than 5%. Therefore, it is observed that the selection of F^{EWE} plays a key role in the selection of lines to place underground.

2) Case II: The wind profiles shown in Fig. 4 are scaled-up and -down by 2%. The results are presented in Tables IV and V.

TABLE VI
COMPUTATIONAL TIME FOR CASES I AND II

π_{thres} (%)	Time (h)		
	Case I	*Case II* (scaled-down)	*Case II* (scaled-up)
1	1.545	0.826	2.186
3	0.788	0.565	0.845
5	0.016	0.021	0.023
7	-	-	0.010

When the wind profiles are scaled-up, as for *Case I*, when the proposed method is applied the total cost decreases compared to when no lines are placed underground. Furthermore, it is observed that when the HEWEs are of higher intensity the minimum total cost is detected for π_{thres} lower than 5%. When the wind profiles are scaled-up, the line failure probabilities, as well as the period of time during which the line failure probabilities are higher than π_{thres}, increase. As a result of the higher line failure probabilities, when no lines are placed underground the total cost increases by 100% compared to *Case I*. Additionally, it is observed that for π_{thres} equal to 7%, three lines are selected to be placed underground, while for *Case I* no lines are selected.

When the wind profiles are scaled-down, the lowest total cost is observed for π_{thres} equal to 5%, while the total cost for π_{thres} equal to 1% and 3% is higher than the total cost when no lines are placed underground. This shows that as the intensity of the HEWEs decreases less lines are needed to be placed underground. Moreover, it is observed that different lines are selected for π_{thres} equal to 1% and 3% compared to *Case I*, where the same lines are selected.

Table VI shows the computational time of the optimization problem for Cases *I* and *II*. It is noted that this the computational time when the subproblems are not solved in parallel at each iteration of the decomposition algorithm. Therefore, the computational time can be reduced further by applying parallel programming techniques.

It is observed that as π_{thres} decreases or wind speed increases the computational time increases. This happens as more line failure scenarios are considered. The execution time when the wind profiles are scaled-up and π_{thres} is equal to 1% is 2 hours and 12 minutes which is considered satisfactory for planning decisions.

3) Case III: Different probabilities of a future EWE to be similar with one of the HEWEs are examined in *Case III*. The probabilities pr_e are considered equal to 0.2, 0.3, 0.05, 0.35 and 0.1 for HEWEs 1-5 presented in Fig. 4, respectively. The results for the scaled-up wind profiles by 2% are presented in Table VII. The total cost is lower than when no lines are placed underground for all the values of π_{thres}. If the objective is the total cost minimization, then the π_{thres} should be selected equal to 5%. However, if the objective is to minimize load shedding, the π_{thres} should be selected equal to 1%. Compared to *Case II*, for π_{thres} equal to 1%, the lines B3-B9 and B11-14 that are detected only within the vulnerable area of HEWE 3 are not selected, as the probability of a future EWE to be similar to HEWE 3 is very low. On the contrary, the line B15-B24 is selected which is located within the vulnerable areas of HEWEs 2 and 3.

TABLE VII
SMC SIMULATION RESULTS FOR CASE III WHEN $F^{EWE} = 4$ (WIND PROFILES SCALED-UP BY 2%)

π_{thres} (%)	Underground Lines	Investment Cost ($\$ \times 10^7$)	LS Cost ($\$ \times 10^7$)	SMC Iter. with LS (%)	Total Cost ($\$ \times 10^7$)
1	B1-B5, B4-B9, B6-B10, B7-B8, B11-B13, B14-B16, B15-B21, B15-B24	10.795	0	0	10.795
3	B1-B5, B4-B9, B6-B10, B7-B8, B11-B14, B14-B16, B15-B21, B15-B24	10.531	0.010	0.8	10.571
5	B1-B5, B6-B10, B7-B8, B15-B16	2.990	1.081	25.8	7.314
7	B6-B10, B7-B8	1.661	1.432	30.4	7.389
> 7	-	-	3.724	43.2	14.896

TABLE VIII
SMC SIMULATION RESULTS FOR STOCHASTIC OPTIMIZATION WHEN $F^{EWE} = 4$ (WIND PROFILES SCALED-UP BY 2%)

Number of scenarios	Underground Lines	Investment Cost ($\$ \times 10^7$)	LS Cost ($\$ \times 10^7$)	SMC Iter. with LS (%)	Total Cost ($\$ \times 10^7$)
40	B4-B9, B6-B10, B7-B8, B11-B14, B14-B16, B15-B21	7.553	0.439	4.4	9.307
30	B3-B9, B4-B9, B6-B10, B7-B8, B14-B16, B15-B21	6.475	0.7669	5.0	9.543
20	B3-B9, B4-B9, B6-B10, B7-B8, B12-B13, B14-B16, B15-B21	8.658	0.298	4.2	9.852

TABLE IX
COMPUTATIONAL TIMES OF PROPOSED METHOD AND STOCHASTIC OPTIMIZATION FOR CASE III

Stochastic Optimization		Proposed Method	
Number of scenarios	Time (h)	π_{thres} (%)	Time (h)
40	5.764	**1**	1.943
30	3.491	**3**	0.917
20	1.475	**5**	0.129
-	-	**7**	0.114

The performance of the proposed method in terms of effectiveness and computational time is compared with a stochastic optimization model. The scenario generation and reduction methodology proposed in [35] is used to produce the representative scenarios. The underground lines determined by the stochastic optimization are used as input to the SMC simulation, to calculate the expected load shedding. The results of the stochastic optimization concerning different number of representative scenarios are shown in Table VIII. The computational times of the proposed method and of the stochastic optimization are presented in Table IX.

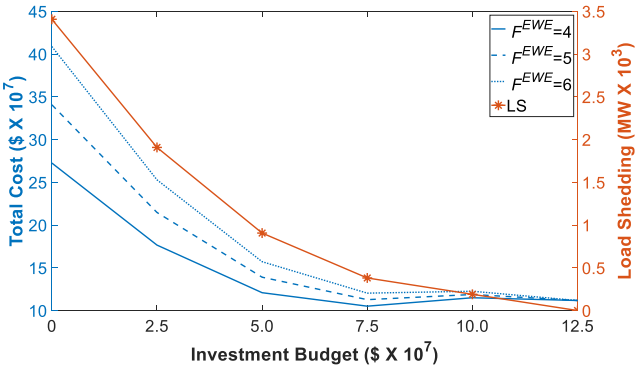

Fig. 5. Total cost and load shedding for different investment budgets when the wind profiles are scaled-up by 2% and π_{thres} is equal to 1%.

It is observed that as the number of representative scenarios increases, the total cost decreases. Regarding the total cost, the stochastic problem provides a better solution compared to the proposed method for π_{thres} equal to 1% and 3%. However, for π_{thres} equal to 5% and 7%, the proposed method provides a better solution in terms of total cost. Additionally, the computational time of the stochastic optimization increases rapidly as the number of representative scenarios increases. The computational time for 40 scenarios is almost 6 hours, while the computational time of the proposed method for π_{thres} equal to 1%, for which value the highest number of possible scenarios is taken into account, is 2 hours. For π_{thres} equal to 5%, when the best solution is provided, the proposed method provides a solution 44 times faster than the stochastic optimization for 40 representative scenarios. For this number of scenarios, the best solution of the stochastic optimization is provided. The computational time of the proposed method could be further reduced by parallel solution of the subproblems at each iteration of the decomposition algorithm.

It is noted that the quality of the solution of the stochastic optimization depends heavily on the representative scenarios. Another method of producing the representative scenarios might provide a better solution. The development of such a method is out of scope of this paper.

Another advantage of the proposed method compared to the stochastic optimization is that it allows the system operator to compare the total cost and the amount of load shedding for different values of π_{thres} and select the optimal solution taking into account both criteria. For instance, if the total cost for a π_{thres} value is slightly higher than the total cost of a higher π_{thres} value, but the amount of load shedding is significantly lower, the system operator could select the solution resulting in a higher total cost with better resilience.

4) Case IV: The variation of total cost and load shedding as a function of investment budget, D, when the wind profiles are scaled-up by 2% and π_{thres} is equal to 1%, is illustrated in Fig. 5. The results are presented for different values of F^{EWE}. The load shedding presented in Fig. 5 corresponds to the occurrence of one EWE. For instance, when $F^{EWE}=$ 4, the load shedding should be multiplied by 4 in order to calculate the total load shedding during the examined planning horizon.

As it was expected, as D increases, the load shedding decreases, as more lines are placed underground. When $D = \$12.5 \times 10^7$, the load shedding is zero, therefore the investigation of a higher budget does not have any value.

The selection of the optimal investment budget depends on F^{EWE} and whether the system operator aims to minimize total cost or load shedding. For $F^{EWE}=$ 4 the lower total cost is detected when the $D = \$7.5 \times 10^7$, while for $F^{EWE}=$ 5 and $F^{EWE}=6$ it is detected when $D = \$12.5 \times 10^7$. However, only when $D = \$12.5 \times 10^7$ no load shedding is detected for all values of F^{EWE}. Hence, the system operator should take into account the uncertainty regarding the estimated number of EWEs and the variation of load shedding and total cost as a function of the investment budget.

TABLE X
LINES EXPOSED TO EACH HEWE – IEEE 118 BUS SYSTEM

HEWE	Vulnerable lines
1	B5-B6, B6-B7, B4-B11, B5-B11, B11-B12, B7-B12, B11-B13, B12-B16, B8-B30, B29-B31
2	B27-B28, B28-B29, B17-B31, B29-B31, B31-B32, B27-B32, B32-B113, B32-B114, B27-B115, B114-B115
3	B19-B20, B20-B21, B21-B22, B22-B23, B23-B25, B25-B26, B25-B27, B26-B30, B23-B32, B30-B38
4	B18-B19, B15-B19, B15-B33, B19-B34, B35-B36, B35-B37, B33-B37, B30-B38, B12-B117,
5	B38-B65, B69-B70, B24-B70, B70-B71, B24-B72, B71-B72, B71-B73, B70-B74, B70-B75, B69-B75, B74-B75, B75-B118, B76-B118

TABLE XI
SMC SIMULATION RESULTS FORCASE I WHEN $F^{EWE} = 5$

π_{thres} (%)	Underground Lines	Investment Cost ($ ×10^7)	LS Cost ($ ×10^7)	SMC Iter. with LS (%)	Total Cost ($ ×10^7)
1	B5-B6, B6-B7, B27-B28, B35-B36, B32-B114, B114-B115	4.984	1.442	44.0	12.194
3	B29-B31, B31-B32, B35-B36	4.498	1.735	57.2	13.173
≥5	-	-	2.579	66.4	12.895

B. IEEE 118-Bus System

The IEEE 118-bus system is used to examine the effectiveness and computational efficiency of the proposed method in a larger network. The system is composed of 54 generators, 118 buses and 186 transmission lines. The length of the lines, considered overhead, is computed based on [36]. The five wind profiles presented in Fig. 4 are considered and the lines exposed to them are presented in Table X. The estimated number of future EWEs, F^{EWE}, is considered equal to 5. The probabilities pr_e are assumed equal to 0.2, 0.3, 0.05, 0.35 and 0.1 for HEWEs 1-5, respectively. The investment budget is set at 5 $\times 10^7$ \$. The results for different values of π_{thres} are presented in Table XI.

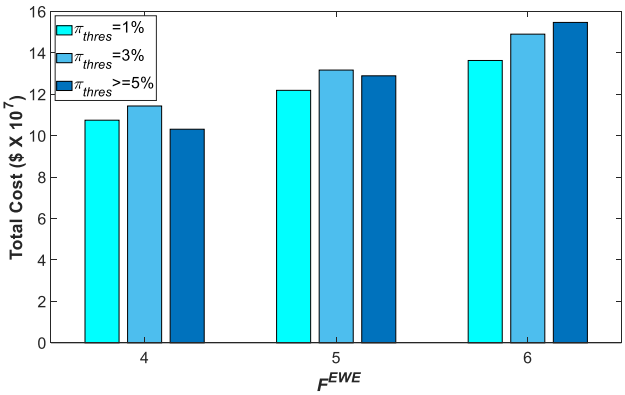

Fig. 6. Total cost for different estimated number of future EWEs.

TABLE XII
COMPUTATIONAL TIME FOR IEEE 118-BUS SYSTEM

π_{thres} (%)	Time (h)
1	4.619
3	1.295

When the π_{thres} is equal or higher than 5%, no line is placed underground. For π_{thres} equal to 1% the total cost is slightly lower than the total cost without line placed underground, while for π_{thres} equal to 3% the total cost is slightly higher. Therefore, the decision of placing the selected lines underground depends heavily on the value of F^{EWE}. Fig. 6 presents the total cost for different values of F^{EWE}. The bars show the total cost for π_{thres} equal to 1%, 3% and equal or higher than 5% (from left to right) for each value of F^{EWE}. It is observed that when F^{EWE}= 4, undergrounding of the lines results in a higher total cost for all the examined values of π_{thres} and therefore it is not economically attractive. However, for higher values of F^{EWE}, when lines are not placed underground, the total cost grows faster due to the higher amount of load shedding. When F^{EWE}= 5, undergrounding of selected lines for π_{thres} equal to 1% leads to a lower total cost. Similarly, when F^{EWE}= 6, undergrounding of selected lines for π_{thres} equal to 3% also leads to a lower cost.

Table XII presents the computational time for π_{thres} equal to 1% and 3%. Even for π_{thres} equal to 1%, the computational time is considered satisfactory for planning. The computational time depends on the complexity of the master problem and the subproblem, which depends on several factors, such as the size of the network, the number of vulnerable lines and the value of π_{thres}, and the number of iterations required for the convergence of the C&CG algorithm. The number of iterations depends on the combination of π_{thres} value and the line failure probabilities. For the IEEE 118-bus system, 6 iterations are required for both values of π_{thres}. In general, as the number of iterations increases, the computational time of the subproblem solution decreases. This is due to the undergrounding of lines and hence the reduction of the number of vulnerable lines. On the contrary, the computational time of the master problem increases, as more worst damage scenarios, identified by the subproblem, are added.

V. CONCLUSION

This paper proposes a framework for the planning of a resilient transmission system against extreme winds. Particularly, a stochastic robust optimization model is presented which determines the lines to be placed underground in order to minimize load shedding in the most cost-efficient way. The probabilities of lines to fail are obtained using wind profiles of HEWEs. Stochastic optimization is used to consider the probability of the future EWEs to be similar with one of the HEWEs under consideration and robust optimization is used to consider the worst damage scenario of each HEWE taking into account only the system degraded states with probability over a predefined threshold. A customized C&CG algorithm is applied to solve the model.

The proposed approach has been illustrated using a modified IEEE Reliability Test System and IEEE 118-bus System and the results prove the effectiveness of the method in selecting the lines to be placed underground reducing the total cost during the planning horizon. The paper provides also a systematic method to select the optimal predefined threshold and investment budget depending on various factors, such as the intensity of the EWEs, the estimated number of EWEs during the planning horizon and the primary objective of system operators, namely to minimize total cost or load shedding. In addition, it is shown that the selection of the investment budget depends on the uncertainty regarding the estimated number of EWEs and whether the system operator aims at the minimization of total cost or load shedding.

REFERENCES

[1] B. Ball, "Rebuilding electrical infrastructure along the gulf coast: A case study," *Bridge-Washington-Nat. Acad. Eng.*, vol. 36, no. 1, Mar. 2006, Art. no. 21.
[2] "Economic benefits of increasing electric grid resilience to weather outages," Washington, DC, USA: Executive Office of the President, Aug. 2013. [Online]. Available: https://www.energy.gov/sites/prod/files/2013/08/f2/Grid%20Resiliency%20Report_FINAL.pdf
[3] J. Walsh *et al.*, "Ch. 2: Our changing climate. climate change impacts in the United States: The third national climate assessment," U.S. Global Change Research Program, 2014. Accessed: Mar. 03, 2021. [Online]. Available: https://nca2014.globalchange.gov/downloads
[4] A. R. Berkeley, III and M. Wallace, "A framework for establishing critical infrastructure resilience goals," Washington, DC, USA, Oct. 2010. [Online]. Available: https://www.dhs.gov/xlibrary/assets/niac/niac-a-framework-for-establishing-critical-infrastructure-resilience-goals-2010-10-19.pdf
[5] N. R. Romero, L. K. Nozick, I. D. Dobson, N. Xu, and D. A. Jones, "Transmission and generation expansion to mitigate seismic risk," *IEEE Trans. Power Syst.*, vol. 28, no. 4, pp. 3692–3701, Nov. 2013.
[6] S. Ma, S. Li, Z. Wang, and F. Qiu, "Resilience-oriented design of distribution systems," *IEEE Trans. Power Syst.*, vol. 34, no. 4, pp. 2880–2891, Jul. 2019.
[7] M. Carrion, J. M. Arroyo, and N. Alguacil, "Vulnerability-constrained transmission expansion planning: A stochastic programming approach," *IEEE Trans. Power Syst.*, vol. 22, no. 4, pp. 1436–1445, Nov. 2007.
[8] M. Panteli, C. Pickering, S. Wilkinson, R. Dawson, and P. Mancarella, "Power system resilience to extreme weather: Fragility modeling, probabilistic impact assessment, and adaptation measures," *IEEE Trans. Power Syst.*, vol. 32, no. 5, pp. 3747–3757, Sep. 2017.

[9] Y. Fang and G. Sansavini, "Optimizing power system investments and resilience against attacks," *Rel. Eng. System Saf.*, vol. 159, pp. 161–173, Mar. 2017.
[10] W. Yuan, J. Wang, F. Qiu, C. Chen, C. Kang, and B. Zeng, "Robust optimization-based resilient distribution network planning against natural disasters," *IEEE Trans. Smart Grid*, vol. 7, no. 6, pp. 2817–2826, Nov. 2016.
[11] H. Zhang, S. Ma, T. Ding, Y. Lin, and M. Shahidehpour, "Multi-stage multi-zone defender-attacker-defender model for optimal resilience strategy with distribution line hardening and energy storage system deployment," *IEEE Trans. Smart Grid*, vol. 12, no. 2 , pp. 1194–1205, Mar. 2020.
[12] M. Ouyang, M. Xu, C. Zhang, and S. Huang, "Mitigating electric power system vulnerability to worst-case spatially localized attacks," *Rel. Eng. Syst. Saf.*, vol. 165, pp. 144–154, Sep. 2017.
[13] A. Bagheri, C. Zhao, F. Qiu, and J. Wang, "Resilient transmission hardening planning in a high renewable penetration era," *IEEE Trans. Power Syst.*, vol. 34, no. 2, pp. 873–882, Mar. 2019.
[14] S. Ma, B. Chen, and Z. Wang, "Resilience enhancement strategy for distribution systems under extreme weather events," *IEEE Trans. Smart Grid*, vol. 9, no. 2, pp. 1442–1451, Mar. 2018.
[15] J. Yan, B. Hu, K. Xie, J. Tang, and H.-M. Tai, "Data-driven transmission defense planning against extreme weather events," *IEEE Trans. Smart Grid*, vol. 11, no. 3, pp. 2257–2270, May 2020.
[16] J. Chang, P. Donohoo-Vallett, P. Ruiz, and T. Brown, "Potential for incorporating climate-related risks into transmission network planning - A review of frameworks and responses preapared for the australian energy market operator," Jun. 2020. [Online]. Available: https://aemo.com.au/-/media/files/major-publications/isp/2020/brattle-group-report.pdf?la=en
[17] M. Yan *et al.*, "Enhancing the transmission grid resilience in ice storms by optimal coordination of power system schedule with pre-positioning and routing of mobile DC de-icing devices," *IEEE Trans. Power Syst.*, vol. 34, no. 4, pp. 2663–2674, Jul. 2019.
[18] I. Kongar, S. Giovinazzi, and T. Rossetto, "Seismic performance of buried electrical cables: Evidence-based repair rates and fragility functions," *Bull. Earthq. Eng*, vol. 15, no. 7, pp. 3151–3181, Jul. 2017.
[19] conEdison, "Climate change vulnerability study," Dec. 2019. [Online]. Available: https://www.coned.com/media/files/coned/documents/our-energy-future/our-energy-projects/climate-change-resiliency-plan/climate-change-vulnerability-study.pdf?la=en
[20] Florida Power & Light Company (FPL), "Storm secure underground pilot program," [Online]. Available: https://www.fpl.com/reliability/storm-secure-underground-program.html
[21] Federal Emergency Management Agency (FEMA), "Using grants to help convert overhead electrical lines to underground," Jul. 2021. [Online]. Available: https://www.hsdl.org/?view&did=13824
[22] European Environment Agency, "Adaptation challenges and opportunities for the european energy system: Building a climate resilient low carbon energy system," LU: Publications Office, 2019. Accessed: Jun. 23, 2021. [Online]. Available: https://data.europa.eu/doi/10.2800/227321
[23] Electric Power Research Institute (EPRI), "Electric power system resiliency - Challenges and opportunities," Feb. 2016. [Online]. Available: https://www.epri.com/research/products/000000003002007376
[24] C. Ning and F. You, "Data-driven stochastic robust optimization: General computational framework and algorithm leveraging machine learning for optimization under uncertainty in the big data era," *Comput. Chem. Eng.*, vol. 111, pp. 115–133, Mar. 2018.
[25] D. N. Trakas and N. D. Hatziargyriou, "Resilience constrained day-ahead unit commitment under extreme weather events," *IEEE Trans. Power Syst.*, vol. 35, no. 2, pp. 1242–1253, Mar. 2020,.
[26] M. Panteli, D. N. Trakas, P. Mancarella, and N. D. Hatziargyriou, "Boosting the power grid resilience to extreme weather events using defensive islanding," *IEEE Trans. Smart Grid*, vol. 7, no. 6, pp. 2913–2922, Nov. 2016.
[27] P. Vincent *et al.*, "Testing and numerical simulation of overhead transmission lines dynamics under component failure conditions," in *Proc. 40th Gen. Session CIGRÉ*, 2004, Art. no. B2-308.
[28] J. M. Eidinger and L. Jr. Kempner, "Reliability of transmission towers under extreme wind and ice loading," in *Proc. 44th Gen. Session CIGRÉ*, 2012, pp. 1–12.
[29] M. Panteli, P. Mancarella, D. N. Trakas, E. Kyriakides, and N. D. Hatziargyriou, "Metrics and quantification of operational and infrastructure resilience in power systems," *IEEE Trans. Power Syst.*, vol. 32, no. 6, pp. 4732–4742, Nov. 2017.
[30] C. Grigg *et al.*, "The IEEE reliability test system-1996. A report prepared by the reliability test system task force of the application of probability methods subcommittee," *IEEE Trans. Power Syst.*, vol. 14, no. 3, pp. 1010–1020, Aug. 1999.
[31] "118 bus power flow test case," Jun. 2021. [Online]. Available: http://labs.ece.uw.edu/pstca/pf118/pg_tca118bus.htm
[32] "BPA transmission services operations & reliability," Jun. 2021. [Online].Available: https://transmission.bpa.gov/Business/Operations/Outages/
[33] M. Kintner-Meyer, J. Homer, P. Balducci, and M. Weimar, "Valuation of electric power system services and technologies," Pacific Northwest National Lab, Richland, Washington, USA, PNNL-25633, 2016.
[34] A. Kargarian and Y. Fu, "System of systems based security-constrained unit commitment incorporating active distribution grids," *IEEE Trans. Power Syst.*, vol. 29, no. 5, pp. 2489–2498, Sep. 2014.
[35] D. N. Trakas, M. Panteli, N. D. Hatziargyriou, and P. Mancarella, "Spatial risk analysis of power systems resilience during extreme events," *Risk Anal.*, vol. 39, no. 1, pp. 195–211, Jan. 2019.
[36] "IEEE 118 bus system." Jul. 2021. [Online]. Available: https://www.pscad.com/knowledge-base/article/29

Dimitris N. Trakas (Member, IEEE) received the Diploma degree in electrical and computers engineering, the M.Sc. degree in energy production and management, and the Ph.D. degree in electrical power engineering from the National Technical University of Athens (NTUA), Athens, Greece, in 2009, 2011, and 2018, respectively. He has worked with the Research, Innovation, and Development Department of the Greek TSO (IPTO) and has participated in the studies for the interconnection of the islands with the National Interconnected Transmission System. He is currently a Senior Researcher with the Smart Rue Research Group, NTUA, Athens, Greece. His research interests include resilience assessment and enhancement of power systems, and TSO-DSO coordination.

Nikos D. Hatziargyriou (Life Fellow, IEEE) received the Diploma degree in electrical and mechanical engineering from the National Technical University of Athens, , Athens, Greece, in 1976, and the M.Sc. and Ph.D. degrees in electrical power engineering from the University of Manchester Institute of Science and Technology, Manchester,U.K., in 1979 and 1982, respectively. He is a Professor of power systems with the National Technical University of Athens, Athens, Greece. He has more than ten year industrial experience as the Chairman and the CEO of the Hellenic Distribution Network Operator and as the Executive Vice-Chair of the Public Power Corporation. He has participated in more than 60 R&D projects funded by the EU Commission, electric utilities and manufacturers for both fundamental research and practical applications. He is author of the book "*Microgrids: Architectures and Control*" (Wiley publications) and of more than 300 journal publications and 600 conference proceedings papers. He was the Chair and Vice-Chair of the EU Technology and Innovation Platform on Smart Networks for Energy Transition (ETIP-SNET). He is an Honorary member of CIGRE and the Past Chair of CIGRE SC C6 "Distribution Systems and Distributed Generation". He is the Past Chair of the Power System Dynamic Performance Committee (PSDPC) and currently the Editor-in-Chief of the IEEE TRANSACTIONS ON POWER SYSTEMS. He is included in the 2016, 2017, and 2019 Thomson Reuters lists of the top 1% most cited researchers. He is 2020 Globe Energy Prize Laureate.